DISPERSAL OF TEPHRA IN EXPLOSIVE ERUPTIONS ON MARS. L. Wilson[1] and J. W. Head[2], [1]Environmental Science Dept., Lancaster Univ., Lancaster LA1 4YQ, UK (l.wilson@lancaster.ac.uk), [2]Dept. of Geological Sciences, Brown Univ., Providence, RI 02912, USA (James_Head@brown.edu).

Introduction: Volcanism has been an important crustal construction process throughout Mars' history [1-2]. Morphologies of early-formed paterae (e.g., Hadriaca, Tyrrhena), together with the presence of fine-grained deposits mantling subjacent cratered terrain [3, 4], suggest that early edifices and deposits were mainly produced by explosive volcanism in contrast to the apparently largely effusive nature of the later shield-building eruptions in Tharsis and Elysium [5-7]. This contrast may be real if high magma volatile contents and/or incorporation of groundwater encouraged the early distinctive explosive eruption style [8-10]. However, an alternative explanation is that decreasing atmospheric pressure may have altered (generally increased) the dispersal of pyroclasts, making it hard to identify the products of many types of geologically young explosive eruptions.

Early theoretical models [11-14] suggested that eruption clouds from long-lived, quasi-steady explosive eruptions should rise much higher on Mars than on Earth for a given mass eruption rate [11]. However, [13] showed that some assumptions made in these models about entrainment of atmospheric gases and internal plume motions are not justified above ~20 km height on Mars, so that clouds from high discharge-rate eruptions, previously expected to convect to much greater heights, cannot do so. To clarify these issues we have (a) reassessed the dispersal of pyroclasts from convecting eruption clouds small enough to be stable, (b) added to previous treatments the consequences of the possible formation of accretionary lapilli within rising eruption clouds, and (c) developed an analysis that shows how volatile rich and high mass-flux eruptions can exploit the low density of the martian atmosphere to produce structures closely resembling the umbrella-shaped plumes on Io, from which pyroclasts, especially those at the coarse end of the expected size range, can be dispersed to significantly greater ranges than from stable convecting eruption clouds.

Sub-surface and near-vent conditions: The inputs to our plume models are a range of magma volatile contents and eruption rates (mass fluxes). For simplicity we treat point-source conduit-type vents rather than fissures. We assume that H_2O dominates exsolved volatiles (others can be converted to equivalent H_2O amounts) with values up to 5 mass %, suggested by estimates up to ~2 mass % H_2O in some SNC meteorites [15] and up to 1.9 mass % H_2O, 5.4 mass % CO_2 (4.1 mass % equivalent H_2O) in some ocean floor alkali basalts/nephelinites on Earth [16]. Mass fluxes span 10^5 to 10^8 kg s^{-1}, covering the entire range observed for all types of mafic eruptions on Earth [17]. The methods given by [17] are used to treat conditions beneath the surface. Under current martian conditions essentially all explosive eruptions are choked at the vent [18, 19] and we decompress the erupted gas/clast mixture adiabatically to atmospheric pressure treating it as a pseudo-gas [18].

Table 1 shows the choked speed, U_v, of gas and small pyroclasts in the vent (it is the same on both planets) as a function of exsolved H_2O mass %, n; and the gas and small pyroclast speeds after decompression to atmospheric pressure on Earth, U_{aE}, and Mars, U_{aM}. As found earlier [11], the speed is approximately proportional to the square root of the exsolved volatile content, and the lower (current) atmospheric pressure on Mars leads to greater speeds there, by a factor varying between 1.3 and 2.

Convecting eruption clouds: Using the starting conditions from Table 1, the resulting eruption clouds are modeled as in [11], derived from [20], for initial conditions leading to cloud heights of up to ~20 km. Tables 2 and 3 show the variations of the radii r of the clouds at their 20 km high tops and the maximum sizes s_{max} of pumiceous pyroclasts that can reach this height. Table 2 shows these variations with exsolved magma water content at a constant mass flux (6×10^5 kg s^{-1}, typical of the 1983 Pu'u 'O'o basaltic fire-fountain eruptions), and Table 3 shows the variations with mass flux at a constant water content of 2 mass %. Clearly the cloud radii, and hence distances from the vent at which clasts are released, vary significantly, but maximum clast sizes could commonly be within less than a factor of 2 of 10 mm. However, by considering the distribution of gas bubble sizes at the pressure level where most magma fragmentation takes place, [11] found that the range of pyroclast sizes available to an eruption cloud, i.e. the range of sizes leaving the vent, was likely to be a few tens of microns to a few mm. Thus most explosive eruption clouds on Mars are capable of transporting somewhat larger clasts to 20 km height than are actually present in the clouds.

In [11] we discussed the combinations of magma volatile content and mass eruption rate that would lead to pyroclastic density currents (surges and ignimbrites) on Mars when eruption clouds failed to incorporate enough atmospheric gas to ensure that they were able to convect in a stable manner. We note here that the new considerations [13] on the inefficiency of atmosphere

entrainment act in the sense of making pyroclastic density current formation more common than thought earlier.

Accretionary lapilli: The much lower atmospheric temperatures on Mars [21] than on Earth suggest that condensation of liquid and then solid H_2O onto pyroclasts will be encouraged, and so we model the formation of accretionary lapilli within rising eruption clouds using [22]. Table 4 shows the variation of the maximum lapillus size that is likely to be formed at the top of a 20 km high cloud as a function of the exsolved magma water content. Accretionary lapilli formation aggregates the smaller pyroclasts into lapilli that may have sizes approaching a maximum of 1 mm.

High mass fluxes and Io-type plumes: If the materials emerging from a volcanic vent do not entrain enough atmospheric gas to influence their motion, they spread out in a ballistic fashion. If they have great enough speeds to punch through the lower atmosphere to the levels (~20 km) where atmosphere interaction is negligible, they have no alternative but to form features similar to the plumes seen on Io [23-25]. Pyroclasts falling back toward the surface re-enter the denser atmosphere at heights of ~20 km and are then subject to wind-driven dispersal as they fall at their terminal velocities in the normal way.

Figure 1 shows the geometry implied, with clasts launched at speed U_{aM} at an angle θ to the vertical on the path $y = (\cos\theta / \sin\theta)\, x - [g / (2\, U_{aM}^2 \sin^2\theta)]\, x^2$ (eq. 1) reaching a maximum height $H = [(U_{aM}^2 \cos^2\theta)/(2\, g)]$ (eq. 2) at a distance $X = [(U_{aM}^2 \sin 2\theta)/(2\, g)]$ (eq. 3) from the vent and then falling back a distance $(H - Z)$ to re-enter the denser part of the atmosphere at height Z above the surface at a radial distance $R = (X + [U_{aM} \sin\theta\, [2(H - Z) / g]^{1/2}])$ (eq. 4) from the vent. It is difficult to predict the maximum angle from the vertical at which pyroclasts will be projected upward, but by analogy with the appearance of eruption plumes on Io, we assume $\theta_{Max} = 30°$ to be an upper limit and also give results for $\theta_{Max} = 10°$. Following the arguments of [13] we take Z as 20 km. The values of the eruption speeds, U_{aM}, of gas and small clasts after decompression to martian atmospheric pressure in explosive eruptions are given as a function of the equivalent exsolved magma water content, n, in Table 1. These are used in Table 5 to find, for each n, the values of H, X, Y and R for each of $\theta = 10°$ and 30°. Table 5 shows that volatile-rich magmas (those with equivalent water contents in excess of ~1.45 mass % if $\theta_{Max} = 10°$ and ~1.9 mass % if $\theta_{Max} = 30°$) can easily project clasts to heights > 20 km, and thus all of these require the non-traditional treatment of the dynamics proposed here.

We argued earlier that a quasi-ballistic treatment will also be required for *any* eruption in which the erupted mass flux dominates the entrained atmosphere mass flux. We use the envelope of the outer edge of the rising ejecta given by (eq. 1) above and the ballistic equations to find the radius r of the eruption "jet" and the speed U of the pyroclasts as a function of height, and then evaluated the total mass flux of atmosphere being entrained [26] by integrating the local fluxes over all heights, where local flux = (~$0.065\ U\ \pi\ r^2 \times$ atmosphere density). The Mars atmosphere model of [21] is used for the gas density. This treatment overestimates atmosphere inflow because, if the ballistic model is applicable, pyroclasts falling back through the atmosphere will interfere with radial air inflow [27]. Thus we feel safe in defining the critical lower limit on the erupted mass flux, M_{crit}, at which this model is applicable as the erupted flux at which the atmosphere inflow just equals the erupted flux. Values of M_{crit} are given in Table 5. These mass fluxes lie in the range that, on Earth, spans the Pu'u 'O'o 1983 basaltic fire-fountain eruptions through the Laki eruption to the Mt. St. Helens 1980 event.

In summary, under current Mars atmospheric conditions, pyroclasts from volatile rich (exsolved equivalent H_2O contents > ~2 mass %) eruptions on Mars having mass eruption rates comparable to or greater than the Laki eruption on Earth will form Io-type plumes and reenter the dense lower atmosphere at radial distances from the vent of at least several tens of km and possible up to ~100 km.

Pyroclast dispersal results: We have used standard treatments [11, 20] of atmospheric drag forces to find the terminal velocities of clasts as a function of height in the martian atmosphere and to then compute the lateral travel distances of clasts with the range of sizes likely to be present in stable eruption clouds reaching 20 km. Values are given in Table 6. Windspeeds are taken from the atmosphere model of [21] and range from 40 m s^{-1} at 20 km height to zero at the surface; travel distances are essentially proportional to the wind speed. To the distances in Table 6 must be added the lateral release distances from the cloud edge (r in Tables 2 and 3). The table shows that coarse (several mm to cm-sized) pyroclasts will be transported for less than 10 km downwind from their release point, though this release point could be many tens to 100 km from the vent in an Io-type eruption. In contrast, finer particles can travel for very much greater distances. These will be hundreds of km for ~0.2 mm sizes, common if accretionary lapilli formation coarsens the grain size distribution, but can readily range up to many thousands of km for any fine (tens of micron) clasts not involved in lapilli formation.

Discussion: (a) Observations (Figure 2) at the Barnhill outcrop at Home Plate in Gusev Crater [28] show an ~4 cm clast that has formed a bomb sag. The size of this clast is at the very top of the range expected for juvenile clasts produced in long-duration, quasi-steady eruptions on Mars like those modeled here, but could be produced in a hydromagmatic explosive eruption. Such a clast could not be transported more than a very few km while falling at its terminal velocity (Table 6), but could have been projected for a few tens of km if ejected in an energetic transient explosion [29]. In either case, it could not possibly have come from Apollinaris Patera (Figure 3), the nearest major volcano to the Spirit landing site, and a closer source vent must be sought. (b) Accretionary lapilli scavenge H_2O from an eruption cloud and emplace it as ice in the fall deposit instead of dispersing it into the atmosphere, with implications for subsequent chemical and morphological evolution of the deposit [30]. (c) If the atmospheric pressure on Mars had been higher in the past, e.g. similar to that of Earth today, this would have influenced all aspects of the eruption process (eruption speed, clast size distribution at the vent, maximum stable cloud rise height, clast fall speed, and wind patterns); dispersal of small clasts would have been greater, but only by a factor of order two, not by orders of magnitude. (d) The results in Table 5 have implications for fire-fountain eruptions on Mars: if the range of mass fluxes in basaltic eruptions is similar to that on Earth, ~0.5 to 1×10^6 kg/s, then in all such eruptions with exsolved equivalent H_2O contents up to ~0.4 mass %, pyroclasts will suffer minimal interaction with the atmosphere, and will form optically dense, heat-conserving fire-fountains from which falling clasts will coalesce into rootless lava flows or form vent ponds feeding flows. This may explain the preponderance of lava flows formed under current atmospheric conditions, in which explosive activity should be common.

References: [1] Carr, M. (2006) *The Surfce of Mars*, Cambridge. [2] Tanaka, K.L. et al. (1992) pp. 345-382 in *Mars*, ed. H. H. Kieffer, et al., Univ. Ariz. Press. [3] Grant, J.A. and Schultz, P.H. (1990) *Icarus, 84*, 166-195. [4] Moore, J.M. (1990) *JGR, 95*, 14279-14289. [5] Carr, M.H. (1973) *JGR, 78*, 4049-4062. [6] Greeley, R. and Spudis P.D. (1981) *Rev. Geophys. Space Phys., 19*, 13-41. [7] Greeley, R. et al. (2000) pp. 75-112 in *Environmental Effects on Volcanic Eruptions: From Deep Oceans to Deep Space*, ed. J.R. Zimbelman, T.K.P. Gregg, Kluwer. [8] Greeley, R. and Crown, D.A. (1990) *JGR, 95*, 7133-7149. [9] Crown, D.A. and Greeley, R. (1993) *JGR, 98*, 3431-3451. [10] Robinson, M.S. et al. (1993) *Icarus, 104*, 301-323. [11] Wilson, L. and Head, J.W. (1994) *Rev. Geophys., 32*, 221-264. [12] Hort, M and Weitz, C.M. (2001) *JGR, 106*, 20547-20562. [13] Glaze, L.S. and Baloga, S.M. (2002) *JGR, 107*, doi: 10.1029/2001JE001830. [14] Kieffer, S.W. (1995) *Science, 269(5229)*, 1385-1391. [15] McSween, H.Y. et al. (2001) *Nature, 409*, 487-490. [16] Dixon, J.E. et al. (1997) *J. Petrol., 38*, 911-939. [17] Wilson, L. and Head, J.W. (1981) *JGR, 86*, 2971-3001. [18] Kieffer, S.W. (1982) pp. 143-157 in *Explosive Volcanism: Inception, Evolution and Natural Hazards*, ed. F.R. Boyd, N.A.S. Press. [19] Mitchell, K.L. (2005) *JVGR., 143*, 187-203. [20] Wilson, L. and Walker, G.P.L. (1987) *G. J. R. Astron. Soc, 89*, 657-679. [21] Moudden, Y. and McConnell, J.C. (2005) *JGR, 110*, doi: 10.1029/2004JE002354. [22] Gilbert, J.S. and Lane, S.J. (1994) *Bull. Volcanol., 56*, 398-411. [23] Cataldo, E. et al. (2002) *JGR, 107*, (E11), doi:10.1029/2001JE001513. [24] Geissler, P. E. (2003) *Ann. Rev. Earth Planet. Sci.*, *31*, 175-211. [25] Zhang, J., *et al.* (2003) *Icarus*, *163*, 182-197. [26] Sparks, R.S.J. et al. (1997) Ch. 2 in *Volcanic Plumes*, Wiley. [27] Ernst, G.G.J. et al. (1996) *JGR, 101*, 5575-5589. [28] Ennis M.E. *et al*. (2007) *LPSC XXXVIII*, abstr. no. 1966. [29] Fagents, S.A. and Wilson, L. (1996) *Icarus*, *123*, 284-295. [30] Fassett, C. I. and Head, J. W., Layered mantling deposits in northeast Arabia Terra, Mars: Noachian-Hesperian sedimentation, erosion and terrain inversion, *JGR*, 2006JE002875, in review, 2007.

Table 1. Conditions in and above explosive vents as a function of exsolved magma H_2O content, n. U_v is choked speed leaving vent; U_{aE} and U_{aM} are speed after decompressing to local atmospheric pressure on Earth and Mars, respectively.

n/mass %	0.1	0.3	0.5	1	2	3.5	5
U_v/(m s^{-1})	35	61	79	112	158	209	250
U_{aE}/(m s^{-1})	46	104	146	227	344	475	577
U_{aM}/(m s^{-1})	95	176	234	340	488	642	756

Table 2. Eruption cloud radii at 20 km height, r, and size of largest pumice that can reach this height, s_{max}, as a function of exsolved magma H_2O content, n, at a constant mass flux of 6×10^5 kg s^{-1}. Eruption cloud with 0.1 mass % H_2O collapses forming pyroclastic density currents.

n/mass %	0.1	0.3	0.5	1	2	3.5	5
r/km	-	2.50	2.58	2.65	2.70	2.75	2.80
s_{max}/mm	-	10.0	10.8	11.2	11.7	12.3	12.9

Table 3. Eruption cloud radii at 20 km height, r, and size of largest pumice that can reach this height, s_{max}, as a function of exsolved magma H_2O content, n, at a constant exsolved H_2O content of 2 mass %.

M/(kg s^{-1})	10^5	10^6	10^7
r/km	6.2	7.9	14.5
s_{max}/mm	3.7	10.8	14.2

Table 4. Maximum sizes, D, of accretionary lapilli formed in 20 km high eruption clouds as a function of exsolved magma H_2O content, n.

n/mass %	0.1	0.3	0.5	1	2	3.5	5
D/mm	0.90	0.75	0.72	0.69	0.69	0.71	0.73

Table 6. Downwind travel distances R of clasts with diameters s released from 20 km height.

s/mm	2	1	0.5	0.2	0.1	0.05	0.02
R/km	10	23	94	585	2340	9360	58500

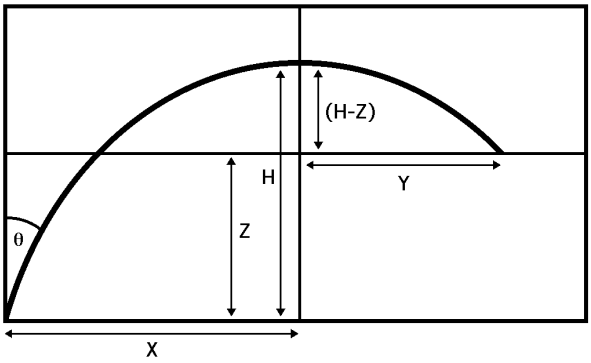

Figure 1. Geometry of quasi-ballistic model.

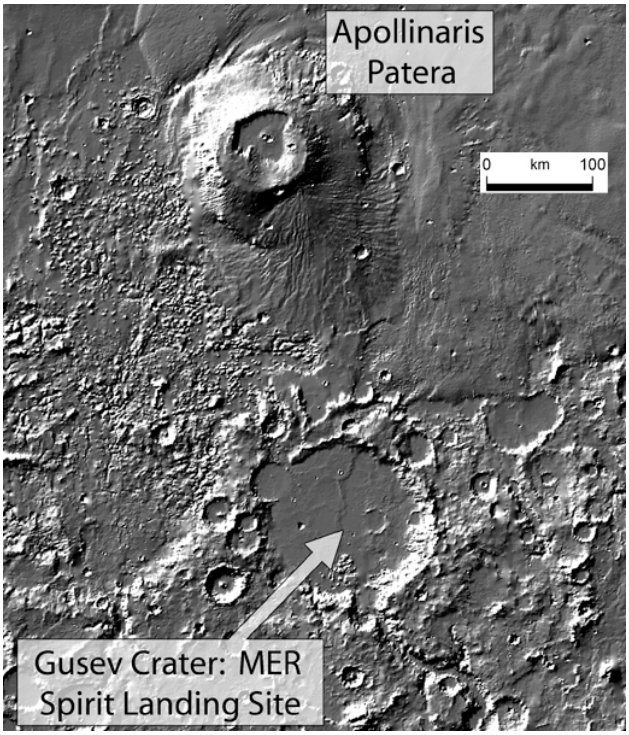

Figure 3. Gusev crater and Apollinaris Patera.

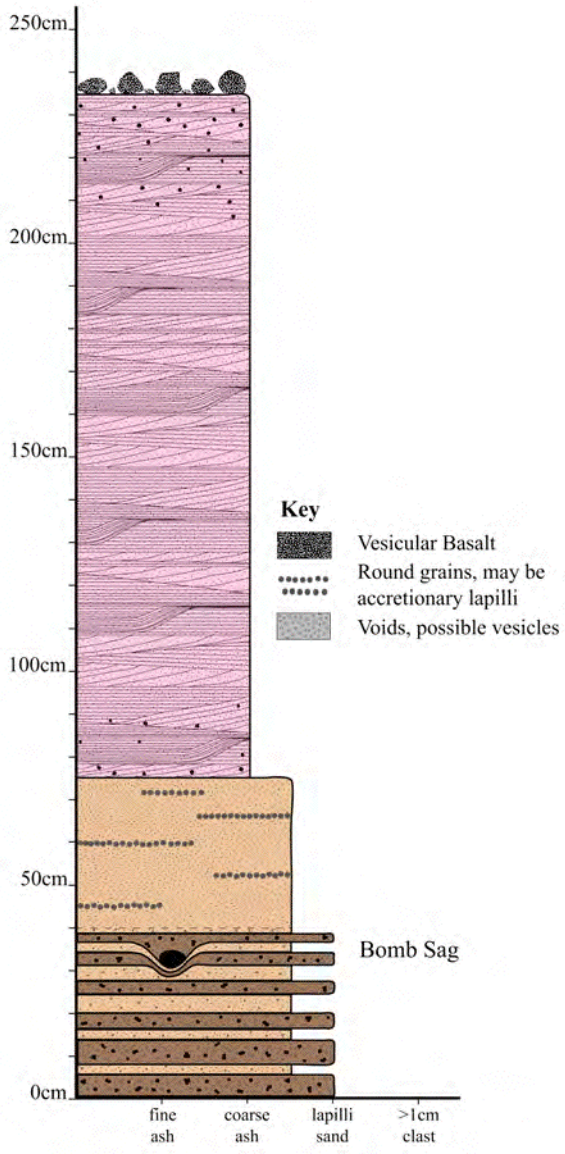

Figure 2. Bomb and bomb-sag in Gusev crater [28].

Table 5: Parameters of quasi-ballistic eruption plumes (see Fig. 1) on Mars. Parameters are defined in the text. A blank entry means that the ~20 km height where the gas laws break down is not reached.

		values for $\theta_{Max} = 10°$					values for $\theta_{Max} = 30°$				
n	U_{aM}	M_{crit}	H	X	Y	R	M_{crit}	H	X	Y	R
mass %	(m s^{-1})	kg/s	km	km	km	km	kg/s	km	km	km	km
0.1	95	3.0×10^4	1.2	0.4			3.6×10^4	0.9	1.1		
0.3	176	6.0×10^5	4.0	1.4			1.2×10^6	3.1	3.6		
0.5	234	2.2×10^6	7.1	2.5			4.8×10^6	5.5	6.4		
1.0	340	1.0×10^7	15.1	5.3			2.4×10^7	11.7	13.5		
1.5	421	2.3×10^7	23.1	8.2	2.99	11.13	5.5×10^7	17.9	20.6		
2.0	488	3.2×10^7	31.0	11.0	6.53	17.48	8.5×10^7	24.0	27.7	11.3	39.0
3.5	642	4.6×10^7	53.7	19.0	15.01	33.96	1.3×10^8	41.5	48.0	34.6	82.5
5.0	756	5.6×10^7	74.5	26.3	22.47	48.75	1.6×10^8	57.6	66.5	53.8	120.3